

Investigating the Effects of Expansion Equal Channel Angular Extrusion (Exp-ECAE) on Dynamic Behavior of AA7075 Aluminum Alloy

J. Shahbazi Karami

Department of Mechanical Engineering,
University of Shahid Rajae Teacher Training, Iran
E-mail: Shahbazi.mech@gmail.com

S. Sepahi-Boroujeni

Department of Mechanical Engineering,
University of Bu-Ali Sina, Iran.
E-mail: saeid_sepahi@yahoo.com

M. Khodsetan *

Department of Mechanical Engineering,
University of Tehran, Iran
E-mail: m_khodsetan@ut.ac.ir

*Corresponding author

Received: 26 February 2016, Revised: 2 April 2016, Accepted: 8 June 2016

Abstract: Expansion equal channel angular extrusion (Exp-ECAE) is a severe plastic deformation (SPD) operation for processing bulk materials. In the current study, AA7075 Al was SPD-processed by expansion equal channel angular extrusion (Ex-ECAE) at various temperatures and ram velocities. Then, using split Hopkinson pressure bar (SHPB), the severely deformed products were compressed at room temperature and strain rates of 0.1~3000 s⁻¹. Both the strain rate sensitivity (SRS) and the apparent activation volume (AAV) were determined for all deformed samples. The results revealed that the Ex-ECAE operation has noticeably increased the SRS. The tensile strength at a strain rate of 3000 s⁻¹ was 6 times increased by conducting Ex-ECAE at 100 °C and with a ram velocity of 7 mm/min. Ex-ECAE was also capable of considerably decreasing the AAV. The results showed the yield stress of both the Exp-ECAE and the annealed samples increased with increasing the strain rate. Also, the results showed that after the Exp-ECAE process, the AAV reached to 6.3 b³ from the initial values of 118.5 b³ in the annealed state.

Keywords: AA7075 Aluminum Alloy, Dynamic Behavior, Expansion Equal Channel Angular Extrusion, Hopkinson Pressure Bar, Severe Plastic Deformation

Reference: J. Shahbazi Karami, S. Sepahi-Boroujeni and M. Khodsetan, "Investigating the Effects of Expansion Equal Channel Angular Extrusion (Exp-ECAE) on Dynamic Behaviour of AA7075 Aluminium Alloy", Int J of Advanced Design and Manufacturing Technology, Vol. 9/No. 3, 2016, pp. 11-18.

Biographical notes: **J. Shahbazi Karami** received his MSc in manufacturing and production engineering from Shahid Rajae University. He is currently PhD student at Shahid Rajae University. His research interests are Hydroforming and gas forming processes. **S. Sepahi-Boroujeni** received his MSc in Mechanical engineering at University of Bu-Ali Sina. His research interests are SPD processes. **M. Khodsetan** received his MSc in Mechanical engineering from University of Tehran. His research interests are traditional and advanced metal forming processes and SPD processes.

1 INTRODUCTION

Based on the Hall-Petch (H-P) relation, the finer the grain size, the higher is the materials' strength. Accordingly, grain refinement has been considered as an efficient way for obtaining products with improved mechanical properties. Recently, studies revealed that not only the metals' strength, but other physical features such as formability, superplasticity, and conductivity could be enhanced through the grain refinement as well. Moreover, many drawbacks such as paradox of strength and ductility can be resolved as the grain size reduces to the nanometer range. Severe plastic deformation processes are the most renowned method to obtain ultra-fine grained (UFG) structures [1]. These processes have been vastly developed for different materials and geometries [2], [3]. Today, aluminum alloys are widely employed in almost all industries. Some unique features such as considerable formability and corrosion resistance have left many industries with no alternative but to utilize such alloys. Due to possessing considerable amounts of Zn, 7000 series aluminum alloys have high strength comparable to that of some steels.

Apart from the magnitude of loading, the rate associated with loading also plays a pivotal role in mechanical behavior of materials [4]. Components and metallic structures are inevitably subjected to the loadings applied with a wide range of deformation rates. Consequently, metals' behavior at high strain rates has attracted much research effort. It should be mentioned that both the strain rate sensitivity (SRS) and rate-controlling mechanism could change by decreasing the grain size [5]. During loading at low and medium strain rates, grain sliding that usually occurs at grain boundaries is restricted by dislocations. This limitation leads to increase in metals' strength. On the other hand, this phenomenon causes considerable decrease in formability. In deformations at high strain rates, it is expected that other flow mechanisms be activated within the material [6], [7].

Many studies have been carried out on the dynamic behavior of materials at high strain rates [8, 9]. The impacts of the Exp-ECAE process on the dynamic behavior of AA6063 aluminum alloy has also been studied [10]. In the present research, AA7075 aluminum underwent Exp-ECAE process at various temperatures and ram velocities. Dynamic behavior at different strain rates and the SRS were determined experimentally for all samples. In addition, apparent activation (AAV) volume and deformation mechanism were both studied. Also, the variations of SRS and the yield strength with temperature and velocity of the SPD process were investigated.

2 EXPERIMENTAL PROCEDURES

The cylindrical samples of $\text{Ø}15 \text{ mm} \times 120 \text{ mm}$ are made of AA7075 aluminium alloy. Afterwards, the samples were annealed at 500°C for 2.5 h to achieve homogeneous

microstructure. Samples, then, underwent Exp-ECAE process at different temperatures and ram velocities according to Table 1. In the design of experiments which was carried out based on the response surface methodology (RSM), temperature and deformation velocity were considered to be design parameters. Design was done in one block with $\alpha = \sqrt{2}$. A total number of 9 experiments were designed with a midpoint for the Exp-ECAE process.

As shown in Fig. 1 the Exp-ECAE die includes a couple of perpendicular channels with diameter of 15 mm, intersecting at a spherical cavity with diameter of 23 mm. In fact, the presence of this spherical cavity distinguishes the Exp-ECAE die geometry from that of the ECAE method [11]. In comparison to the ECAE, in the Exp-ECAE process the expansion of material in the cavity introduces an extra plastic strain which contributes to improvement of mechanical properties. The edge radius at the intersection of channels and sphere is 1 mm and there is an offset of 2 mm between the center of spherical hollow and the centerlines of channels. Reducing the interfacial friction, MoS_2 was implemented as the lubricant. Cylindrical heaters were used in order to elevate die temperature. The temperature was monitored by a thermocouple placed near the spherical cavity and controlled manually with a 5°C tolerance. To ensure thermal equilibrium between the die and the billet, the billet was placed in the inlet channel 10 min prior to the beginning of process.

Table 1 Temperatures and ram velocities in the Ex-ECAE process designed by RSM.

| Test number | Ex-ECAE Process temperature ($^\circ\text{C}$) | Ex-ECAE Process speed (mm/min) |
|-------------|--|--------------------------------|
| 1 | 100 | 7 |
| 2 | 120 | 4 |
| 3 | 120 | 10 |
| 4 | 175 | 2.8 |
| 5 | 175 | 7 |
| 6 | 175 | 11.2 |
| 7 | 230 | 4 |
| 8 | 230 | 10 |
| 9 | 230 | 7 |

After the Exp-ECAE process, the samples were prepared for quasi-static and dynamic compression tests. The compression tests were designed in a way that the loading direction was uni-axial and parallel to the flow direction in the Exp-ECAE process. For quasi-static compression tests, cylindrical samples with diameter of 6 mm and a length to diameter ratio of 1.5 were machined from both the processed and the annealed samples.

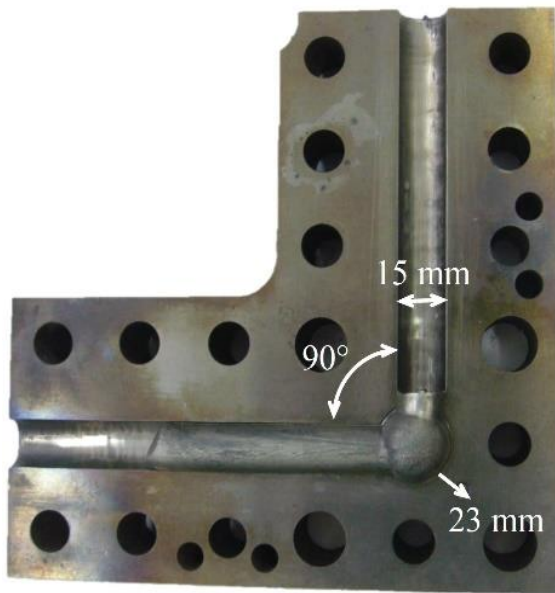


Fig. 1 One half of the Exp-ECAE die and the partially deformed component

The samples of compression tests were machined from the middle part of the Exp-ECAE products so that their centerlines were coincident with that of the initial billets. The tests were conducted at the strain rate of 0.1 s^{-1} .

Reducing the friction between the samples and the grippers of the test machine, MoS_2 was used as a lubricant. Samples of 5 mm both in diameter and length were prepared for dynamic experiments out of processed and annealed billets. Split Hopkinson pressure bar (SHPB) machine was used to carry out the high-strain tests. In addition to the gas gun, striker bar, incident bar, and transmission bar are other main components of the test machine. The striker bar was shot toward the incident bar via the gas gun. With the collision of these bars, an elastic compressive stress wave was emitted in the longitudinal direction of the incident bar toward the sample.

Once this wave arrives at the sample, the plastic deformation of the sample started. Due to impedance difference between the sample and the bars, a part of the wave was reflected and the other part progressed toward the transmission bar. Stress wave was recorded by strain gauges placed on the incident and transmission bars. Assuming the deformation to be homogenous and uniform stress state, according to one-dimensional stress wave theory, applied stress (σ), strain (ϵ), and strain rate ($\dot{\epsilon}$) can be calculated as follows [12]:

Where ϵ_i and ϵ_t are emitted strain pulse and transitional strain recorded by strain-meters on input and output bars, respectively. E and A are the speed of longitudinal wave emission, the Young's modulus, and the cross-section area of input and output bars, respectively.

$$\begin{cases} \sigma = E \left(\frac{A}{A_s} \right) \epsilon_t \\ \epsilon = \frac{2C_0}{l_s} \int_0^t \epsilon_t d\tau \\ \dot{\epsilon} = \frac{2C_0}{l_s} \dot{\epsilon}_t \end{cases} \quad (1)$$

l_s and A_s are the length and the cross-section of the sample, respectively. During the compression tests, the pressure of gas gun was controlled in a way to ensure the application of the approximate strains of $10^2 \sim 3 \times 10^3$.

3 RESULTS AND DISCUSSION

Fig. 2 illustrates voltage-time variations recorded by strain gauges installed on the incident and the transmission bars, i.e. incident bar signal and transmitted bar signal, respectively. This graph corresponds to the compression test conducted at strain of 1200 s^{-1} for the sample processed by Exp-ECAE at 120°C and with a punch velocity of 4 mm/min. As can be seen in this figure, while the stress wave, which propagates through the incident bar, is recorded by corresponding strain gauge, the other strain gauge almost senses no deflection. Once arrives at the transmission bar, the transmitted wave is monitored by the transmission strain gauge. At the same time, that part of the wave which is reflected toward the incident bar is also recorded by the incident strain gauge. Using equations (1), voltage-time pulses are converted to strain-time curves. Stress, strain rate, and strain applied to the sample are then calculated as a function of time. True stress-strain curves can finally be obtained by omission of the time parameter. Dynamic stress-strain graphs are presented in Fig. 3 for both processed and annealed samples. This figure shows the stress-strain behavior of AA7075 aluminum alloy compressed at different strain rates ($10^{-1} \sim 3.2 \times 10^3 \text{ s}^{-1}$). The stress-strain curves obtained for the annealed state (prior to the Exp-ECAE process) is also presented in Fig. 3. As it is evident in this figure, the flow stresses of Exp-ECAE products show considerable increase compared to the annealed samples. Increasing the deformation velocity in the Exp-ECAE process, due to giving rise to larger number of dislocations, is accompanied with grain refinement in the final product. Thus, increase in the Exp-ECAE velocity can strengthen the material's structure. In Fig. 3, the annealed sample presents the lowest strength at different strains. It is obvious that increasing the velocity and reducing the

temperature of Exp-ECAE process leads to increase in the flow stress at different strains. Increase in the impact of strain rate on the flow stress with increasing the velocity and decreasing the temperature is also evident. The annealed sample, on the other hand, shows the least variations with respect to increase in the strain rate.

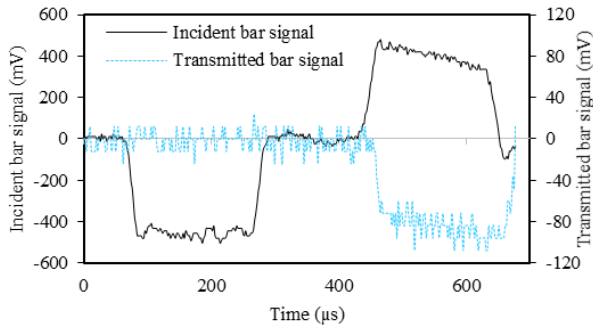
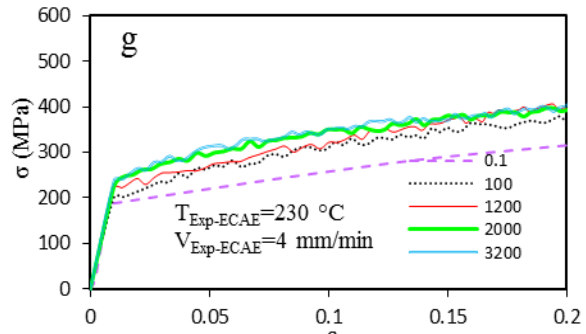
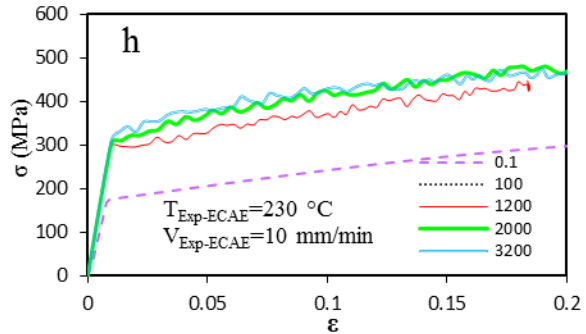
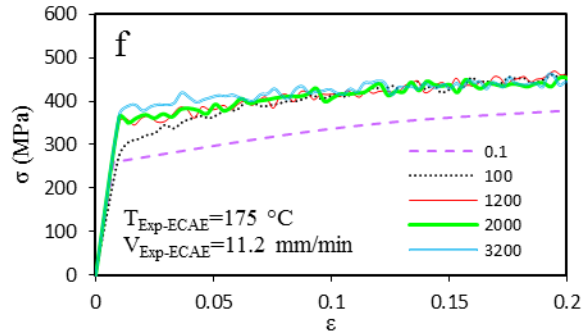
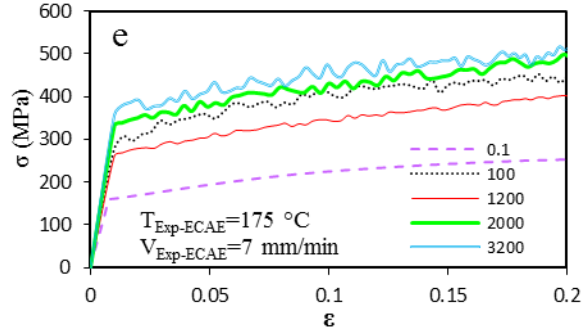
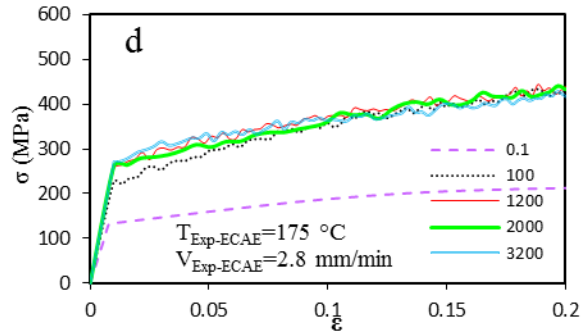
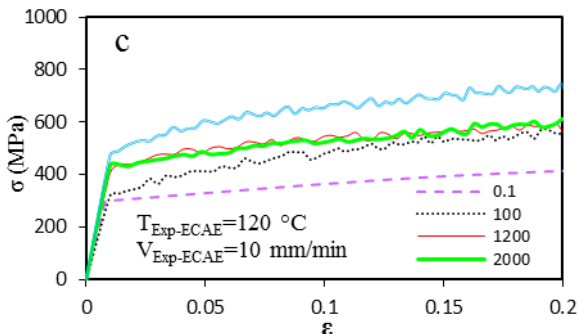
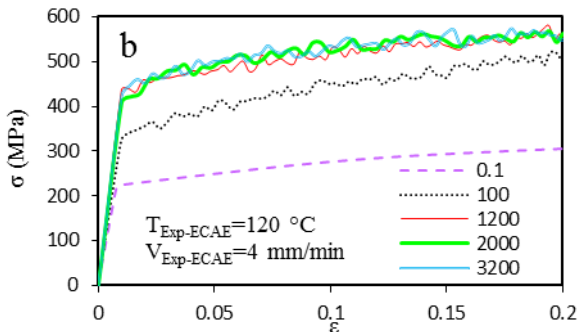
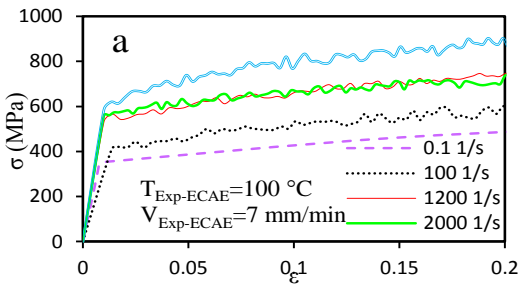


Fig. 2 Incident, reflected, and transmitted pulses recorded at strain rate of 1200 s⁻¹ during the compression of sample underwent Exp-ECAE at 120°C and with a ram velocity of 4 mm/min



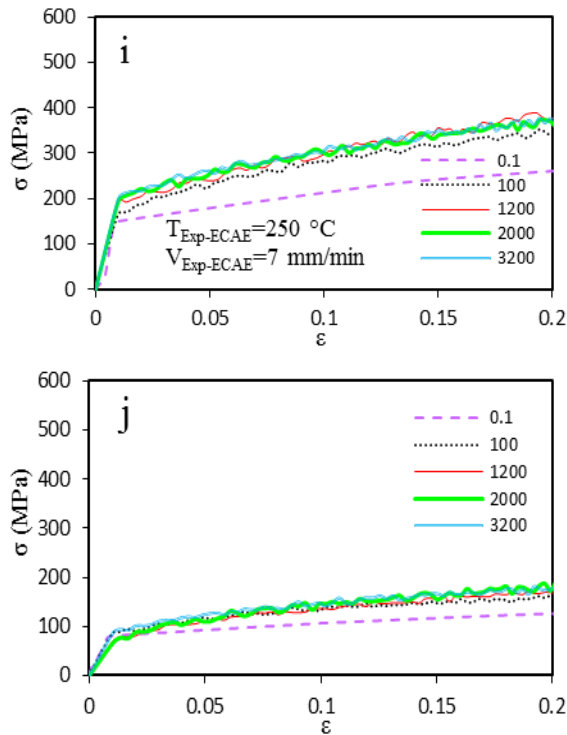


Fig. 3 Compressive stress-strain graphs at strain rates of 0.1 S⁻¹ to 3000S⁻¹ for a-i) Exp-ECAEed products and j) annealed samples

The sample which was severely deformed via the Exp-ECAE at 100°C and with a punch velocity of 7 mm/min has the highest strength at all strain rates. Carrying out the Exp-ECAE process at 250°C and with a ram velocity of 7 mm/min, on the other hand, has led to the lowest strength among processed products.

It can be claimed that increase in dislocation density, which is considered to be one of the major barriers for slip planes, results in the increase in flow stress. In addition, with decreasing the temperature of the process, microstructural recovery and annihilation of dislocations will be decelerated, leading to increase in the flow stress of the sample.

Due to low temperature and relatively high deformation velocity, the sample processed at 100°C and 7 mm/min could have the highest dislocation density among other samples. By increasing the temperature of the process up to 250°C, the density of dislocations could be decreased significantly, leading to a decrease in material's strength at different strain rates.

Nearly in all stress-strain curves, increasing the strain rate up to 3000 s⁻¹, results in a decrease in work hardening of the material. With increasing the strain rate, the rate of dislocation generation in the deformed sample is accelerated [4]. Increasing the density of dislocations is accompanied with increase in dynamic recrystallization [13] and could result in a balance between generation and annihilation rates of dislocations. Therefore, such a restriction on dislocation generation which is caused by dynamic recrystallization

could be held accountable for decrease in work hardening at strain rate of 3200 s⁻¹.

As a matter of fact, the flow stress of a material could be considered as a function of its microstructural characteristics, temperature, and strain rate. Moreover, the microstructure of materials changes in proportion to the amount of applied plastic deformation or plastic strain. Thus, the yield stress can be defined as a function of strain, strain rate and temperature. The SRS can be defined as follows:

$$m = \left(\frac{\partial \ln \sigma}{\partial \ln \dot{\epsilon}} \right)_{T, \epsilon} \quad (2)$$

According to equation (2), in a particular temperature and plastic strain, i.e. in a particular microstructural status, the SRS can be calculated. Here, this parameter is calculated by obtaining the slope of the line fitted to the logarithmic graph of the stress-strain rate at a specific strain [14]. Based on the thermal activation theory, the normal stress for the start of plastic deformation in uniaxial loading is as follows [4]:

$$\sigma = \sigma_a + \sqrt{3} \left[\Delta F - kT \ln \frac{\dot{\epsilon}_0}{\dot{\epsilon}} \right] / V_a \quad (3)$$

In which σ_a is the non-thermal portion of the stress, $\dot{\epsilon}_0$ is the reference normal strain rate, $\dot{\epsilon}$ is the applied strain rate and V_a is apparent activation volume. k , T and ΔF are Boltzmann constant, temperature, and activation energy, respectively. By partial differentiating this equation with respect to the term $\ln \dot{\epsilon}_0$ [4]:

$$\frac{\partial \sigma}{\partial \ln \dot{\epsilon}} = \frac{\sqrt{3}kT}{V_a} \quad (4)$$

According to equation (4), the AAV can be approximated by fitting a line to the stress versus $\ln \dot{\epsilon}_0$ graph. Fig. 4 shows the amounts of SRS and AVV for Exp-ECAE products together with the annealed sample. The SRS prior to the Exp-ECAE process was 0.0343, while it increased to 0.1104, more than threefold increase, after performing the Exp-ECAE at 100°C and with a punch velocity of 7mm/min.

The significant increase in the SRS could be attributed to the increase in dislocation density of the product. This is consistent with the research works conducted on the ECAE process [15]. If in a specific strain, the stress-strain curves are coincided with each other, SRS will be zero. As it was mentioned before, metal forming processes and severe plastic deformation operations in particular, increase the dislocation density of products. At lower temperatures and higher deformation velocities, there are little chances of grain growth and dislocation recovery, resulting in higher

dislocation density in product. Increase in the strain rate will increase the material's resistance to flow and, in other words, SRS will increase. As Fig. 3 depicts, the behavior of samples processed under conditions of $T=100^{\circ}\text{C}$, $V=7$ mm/min and $T=120^{\circ}\text{C}$, $V=7$ mm/min, also confirms this claim. Under these process conditions, due to high process velocity and relatively low temperature, many dislocations are produced within the material, resulting in a significant increase in the strength of product with increasing the strain rate. In higher temperatures and lower velocities, SRS decreases. In other words, the material's behavior shows little variation with increasing the strain rate.

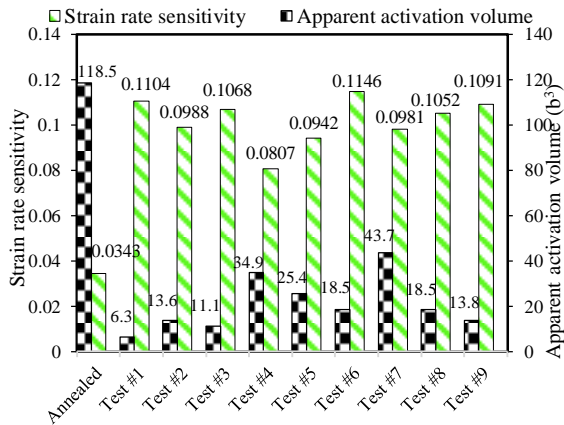


Fig. 4 Strain rate sensitivity and apparent activation volume for the products of Exp-ECAE experiments conducted based on Table 1

With carrying out the Exp-ECAE process, the AAV has significantly decreased. AAV for coarse grained FCC structures is approximately $10^2 \sim 10^3 b^3$ (b is Burgers vector) [5]. This parameter decreases noticeably with decreasing the grain size [4], [16]. For coarse grained metals in which the initiation of material flow depends on the resistance of dislocations to the sliding of slip planes, decreasing the average grain size changes the mechanism of material flow from dislocation movement to the one with lower AAV [17]. Prior to Exp-ECAE process, the AAV was $118.5 b^3$ (for aluminum $b=2.85 \times 10^{-10}$). After the Exp-ECAE process at 100°C and 7 mm/min, this parameter reached $6.3 b^3$. In strain rate of 2000 s^{-1} , stress-strain behavior of billets processed with a ram velocity of 7 mm/min and at different temperatures of 100, 175, and 250°C , is shown in Fig. 5. As can be seen in this figure, the strength of material declines with increasing the deformation temperature. With increasing the temperature, microstructure recovery and dislocation annihilation are accompanied by increasing in the average grain size. Consequently, the material's structure notably weakens which is apparent in Fig. 5.

Considering high amounts of plastic strain inherent in the Exp-ECAE process, the occurrence of the dynamic recrystallization in temperatures below the half of the melting point, is anticipated. Considerable reduction in the strength of products with increasing the process temperature from 175 to 250°C , other than microstructure recovery, could be attributed to the dynamic recrystallization.

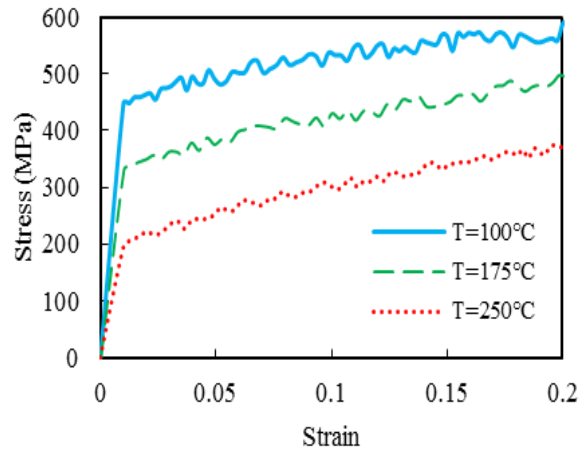


Fig. 5 The stress-strain behavior recorded at strain rate of 2000 s^{-1} for the billets processed with a ram velocity of 7 mm/min and at different temperatures

During the material flow at low strain rates, due to high aggregation of dislocations in grain boundaries, dislocations' movement is disrupted when crossing these locations. This disruption is in a way that a dislocation spends a considerable time on defeating the hindrance. Thus, the time for crossing a barrier, compared to the time which a dislocation spends on being blocked by other dislocations, is negligible. Moreover, for the initiation of material flow in this situation, high activation energy is required to move dislocations [4]. During plastic deformation, as the strain rate increases, other mechanisms can play role in material flow. In viscous-drag mechanism, which occurs in plastic deformations at high strain rates, the time for a dislocation to travel between consecutive barriers is approximately equal to the time that it spends to stay among the barriers. The tension force that is created by stress wave propagation or electron emission accounts for lattice vibration, has a great impact on the flow stress of the material. The lattice vibrations and electrons' movement increase dislocation energy, leading to scattering them in the material. Therefore, the activation energy for the material flow decreases [18]. There is a linear relationship between flow stress and the strain rate [19]. Fig. 6 shows the strain rate- flow stress graph for some of the samples. As can be seen in this figure, by increasing the strain rate, the graphs show more linear trends. Thus, most likely, viscous-drag mechanism governs the dislocation movement.

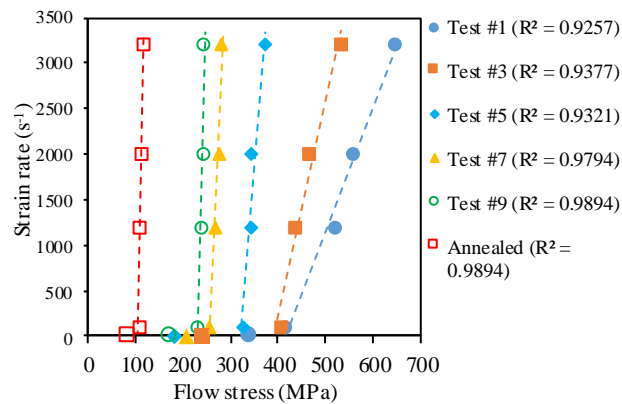


Fig. 6 The strain rate variations versus flow stress in 10% strain for some experiments carried out based on Table 1 as well as for the annealed sample, along with linear fittings for the strain rates above 0.1 s^{-1}

4 CONCLUSION

Dynamic behavior of AA7075 aluminum alloy which was processed via Exp-ECAE at various temperatures and with a vast range of ram velocities was studied by quasi-static and dynamic compression tests. After conducting the Exp-ECAE process, the flow stress of samples increased significantly. Also, with increasing the strain rate, the yield stress of both the Exp-ECAE products and the annealed samples increased, accordingly. The flow stress increased by increasing the velocity and decreasing the temperature of the SPD process. This increase, which is evident in all strain rates, could be attributed to increase in the density of dislocations within the samples. A balance between dislocation generation and dynamic recrystallization, probably, can be held accountable for decrease in work hardening in high strain rates (3200 s^{-1}). The strain rate sensitivity for the sample processed at 100°C and with a punch velocity of 7 mm/min , presented more than threefold increase compared to the annealed sample, which could be due to increase in the density of dislocations. The apparent activation volume was calculated to be $118.5 b^3$ in the annealed state, while reached $6.3 b^3$ after conducting the Exp-ECAE operation at 100°C and with a ram velocity of 7 mm/min . Studies showed that the strain rate sensitivity is proportional to the deformation velocity and inversely proportional to the temperature at which the Exp-ECAE operation is carried out. At higher process temperatures, the strain rate sensitivity decreased with respect to the temperature. The linear trend of the strain rate-flow stress curves determined for AA7075 alloy could be a sign of change in dislocation movement mechanism and activation of the viscous-drag mechanism in the product.

REFERENCES

- [1] Valiev, R. Z., Islamgaliev, R. K. and Alexandrov, I. V., "Bulk nanostructured materials from severe plastic deformation", Progress in Materials Science, Vol. 45, 2000, pp. 103-189.
- [2] Pardis, N., Talebanpour, B., Ebrahimi, R. and Zomorodian, S., "Cyclic expansion-extrusion (CEE): A modified counterpart of cyclic extrusion-compression (CEC)", Materials Science and Engineering: A, Vol. 528, 2011, pp. 7537-7540.
- [3] Torabzadeh, H., Faraji, G. and Zalnezhad, E., "Cyclic Flaring and Sinking (CFS) as a New Severe Plastic Deformation Method for Thin-walled Cylindrical Tubes", Transactions of the Indian Institute of Metals, 2015, pp. 1-6.
- [4] Suo, T., Chen, Y., Li, Y., Wang, C. and Fan, X., "Strain rate sensitivity and deformation kinetics of ECAPed aluminium over a wide range of strain rates", Materials Science and Engineering: A, Vol. 560, 2013, pp. 545-551.
- [5] Meyers, M. A., Mishra, A. and Benson, D. J., "Mechanical properties of nanocrystalline materials", Progress in Materials Science, Vol. 51, 2006, pp. 427-556.
- [6] Ferguson, W. G., Kumar, A. and Dorn, J. E., "Dislocation Damping in Aluminum at High Strain Rates", Journal of Applied Physics, Vol. 38, 1967, pp. 1863-1869.
- [7] Kumar, A., Hauser, F. E. and Dorn, J. E., "Viscous drag on dislocations in aluminum at high strain rates", Acta Metallurgica, Vol. 16, 1968, pp. 1189-1197.
- [8] Chinta Babu, U., Prasad, K. and Kamat, S. V., "Effect of strain rate on tensile behaviour of cryo-rolled ultrafine grained OFHC copper", Transactions of the Indian Institute of Metals, Vol. 64, 2011, pp. 321-324.
- [9] SridharBabu, B., Kumaraswamy, A., and AnjaneyaPrasad, B., "Effect of Indentation Size and Strain Rate on Nanomechanical Behavior of Ti-6Al-4VAlloy", Transactions of the Indian Institute of Metals, Vol. 68, 2014, pp. 143-150.
- [10] Fereshteh-Saniee, F., Sepahi-Boroujeni, S., Lahmi, S. and Majzoubi, G. H., "An Experimental Investigation on the Strain Rate Sensitivity of a Severely Deformed Aluminum Alloy", Experimental Mechanics, Vol. 55, 2015, pp. 569-576.
- [11] Sepahi-Boroujeni S. Fereshteh-Saniee, F., "Expansion equal channel angular extrusion, as a novel severe plastic deformation technique", Journal of Materials Science, Vol. 50, 2015, pp. 3908-3919.
- [12] Kolsky, H., "An Investigation of the Mechanical Properties of Materials at very High Rates of Loading", Proceedings of the Physical Society. Section B, Vol. 62, 1949, pp. 676.
- [13] Krausz, A. S. Krausz, K., "Unified Constitutive Laws of Plastic Deformation", San Diego, California: Elsevier Science, 1996.
- [14] Wei, Q., Jiao, T., Mathaudhu, S. N., Ma, E., Hartwig, K. T. and Ramesh, K. T., "Microstructure and mechanical properties of tantalum after equal channel angular extrusion

- (ECAE)", *Materials Science and Engineering: A*, Vol. 358, 2003, pp. 266-272.
- [15] Valiev, R. Z. Langdon, T. G., "Principles of equal-channel angular pressing as a processing tool for grain refinement", *Progress in Materials Science*, Vol. 51, 2006, pp. 881-981.
- [16] Kapoor, R., Singh, J. B. and Chakravartty, J. K., "High strain rate behavior of ultrafine-grained Al-1.5 Mg", *Materials Science and Engineering: A*, Vol. 496, 2008, pp. 308-315.
- [17] Suo, T., Li, Y. I, Xie, K, Zhao, F., Zhang, K. S. and Deng, Q., "Experimental investigation on strain rate sensitivity of ultra-fine grained copper at elevated temperatures", *Mechanics of Materials*, Vol. 43, 2011, pp. 111-118.
- [18] Wolfer, W. G., "Phonon Drag Dislocations at High Pressures", UCRL-ID-136221; TRN: US0204469, 1999.
- [19] Kumar, A. Kumble, R. G., "Viscous Drag on Dislocations at High Strain Rates in Copper", *Journal of Applied Physics*, Vol. 40, pp. 3475-3480, 1969.